

Scaling Hidden Markov Language Models

Anonymous EMNLP submission

Abstract

The hidden Markov model (HMM) is a fundamental tool for sequence modeling that cleanly separates the hidden state from the emission structure. However, this separation makes it difficult to fit HMMs to large datasets in modern NLP, and they have fallen out of use due to very poor performance compared to fully observed models. This work revisits the challenge of scaling HMMs to language modeling datasets, taking ideas from recent approaches to neural modeling. We propose methods for scaling HMMs to massive state spaces while maintaining efficient exact inference, a compact parameterization, and effective regularization. Experiments show that this approach leads to models that are much more accurate than previous HMMs and n-gram-based methods, making progress towards the performance of state-of-the-art NN models.

1 Introduction

Hidden Markov models (HMMs) are a fundamental latent-variable model for sequential data. Historically they have been used extensively in NLP for tasks such as sequence modeling (Rabiner, 1990), alignment (Vogel et al., 1996), and even, in a few cases, language modeling (Kuhn et al., 1994; Huang, 2011). Compared to other sequence models, HMMs are naturally appealing since they fully separate the process of generating hidden states from observations, while allowing for exact posterior inference.

State-of-the-art systems in NLP have moved away from utilizing latent hidden states and toward deterministic deep neural models. We take several lessons from the success of neural models for NLP tasks: (a) model size is critical for finding better local optima, e.g. large LSTMs (Zaremba et al., 2014) show marked improvements in performance;

(b) the right factorization is critically important for representation learning, e.g. a feedforward model (Bengio et al., 2003) can have the same probabilistic structure as an n-gram model while performing significantly better; (c) dropout is key to achieving strong performance on smaller datasets (Zaremba et al., 2014; Merity et al., 2017).

We revisit HMMs for language modeling, positing that competitive performance may require very large models. Our contributions are as follows: We demonstrate large improvements in an HMM language model by scaling the state space. Towards that goal, we introduce three techniques: a modeling constraint that allows us to use a large number of states while maintaining efficient exact inference, a neural parameterization that improves generalization while remaining faithful to the probabilistic structure of the HMM, and a variant of dropout that both improves accuracy and halves the computational overhead during training.

Experiments employ HMMs on two language modeling datasets. Our three techniques allow us to train an HMM with tens of thousands of states, significantly outperforming past HMMs as well as n-gram models.

2 Related Work

In order to improve the performance of HMMs on language modeling, several recent papers have combined HMMs with neural networks. Buys et al. (2018) develop an approach to relax HMMs, but their models either perform poorly or alter the probabilistic structure to resemble an RNN. Krakovna and Doshi-Velez (2016) utilize model combination with an RNN to connect both approaches in a 20 state model. We instead improve pure HMMs by scaling to many states.

Prior work has considered neural parameteriza-

tions of HMMs. Tran et al. (2016) demonstrate improvements in POS induction with a neural parameterization of an HMM. They consider small state spaces, as the goal was tag induction rather than language modeling.¹

Prior work has also used HMMs with many states. Dedieu et al. (2019) introduce a sparsity constraint in order to train a 30K state HMM for character-level language modeling; however, their constraint precludes application to large vocabularies. We overcome this limitation and train models on word-level language modeling.

Finally, another approach for scaling state spaces is to grow from small to big via a split-merge process (Petrov et al., 2006; Huang, 2011). In particular, Huang (2011) learn an HMM for language modeling via this process. As fixed-size state spaces are significantly easier to optimize for GPUs, we leave split-merge procedures for future work.

3 Background: HMMs

We are interested in learning a distribution over observed tokens $\mathbf{x} = \langle x_1, \dots, x_T \rangle$, with each token x_t an element of the finite vocabulary \mathcal{X} . Hidden Markov models (HMMs) specify a joint distribution over observed tokens \mathbf{x} and discrete latent states $\mathbf{z} = \langle z_1, \dots, z_T \rangle$, with each z_t from finite set \mathcal{Z} . For notational convenience, we define the starting state $z_0 = \epsilon$. This yields the joint distribution

$$p(\mathbf{x}, \mathbf{z}; \theta) = \prod_{t=1}^T p(x_t | z_t) p(z_t | z_{t-1}) \quad (1)$$

The distributions are parameterized as follows

$$p(z_t | z_{t-1}) \propto e^{\psi_{z_{t-1}z_t}} \quad p(x_t | z_t) \propto e^{\phi_{z_t x_t}} \quad (2)$$

with transitions $\psi \in \mathbb{R}^{|\mathcal{Z}| \times |\mathcal{Z}|}$ and emissions $\phi \in \mathbb{R}^{|\mathcal{Z}| \times |\mathcal{X}|}$. We refer to emissions $p(x_t | z_t)$ as \mathbf{O} .

We distinguish two types of parameterizations: *scalar* and *neural*. A scalar parameterization simply uses $\theta = \{\phi, \psi\}$ to fit one model parameter for each distributional parameter ($O(|\mathcal{Z}|^2 + |\mathcal{Z}||\mathcal{X}|)$ model parameters). A neural parameterization uses θ as parameters of a neural network that generates ϕ and ψ , which allows for factorization.

¹ Other work has used neural parameterization for structured models, such as dependency models (Han et al., 2017), hidden semi-Markov models (Wiseman et al., 2018), and context free grammars (Kim et al., 2019).

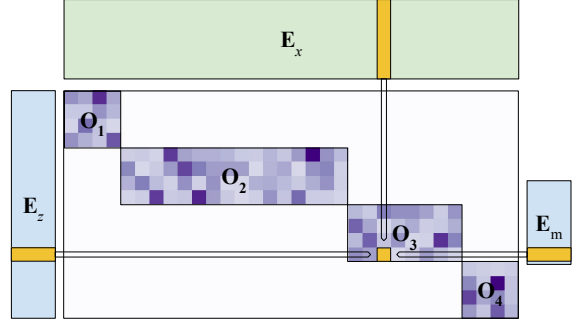


Figure 1: The emission matrix as a set of blocks $\mathbf{O}_1, \dots, \mathbf{O}_4$ with fixed height k . Each active cell is constructed from word \mathbf{E}_x , state \mathbf{E}_z , and block \mathbf{E}_m embeddings.

In order to fit an HMM to data \mathbf{x} , we must marginalize over the latent states to obtain the likelihood $p(\mathbf{x}) = \sum_{\mathbf{z}} p(\mathbf{x}, \mathbf{z})$. This sum can be computed in time $O(T|\mathcal{Z}|^2)$ via dynamic programming, which becomes prohibitive if the number of latent states $|\mathcal{Z}|$ is large. We can then optimize the likelihood with gradient ascent (or alternative variants of expectation maximization).

HMMs and RNNs Recurrent neural networks (RNNs) do not decouple the latent dynamics from the observed. This often leads to improved accuracy, but precludes posterior inference which is useful for interpretability. A further benefit of HMMs over RNNs is that their associative structure allows for parallel inference via the prefix-sum algorithm (Ladner and Fischer, 1980).²

4 Scaling HMMs

Blocked Emissions Efficiency of marginal inference inherently limits the state space of general HMMs. However, we can improve inference complexity in special cases. As states in an HMM are used to represent context, a reasonable assumption is that not every word should be used in every context. Inspired by cloned HMMs (Dedieu et al., 2019), we constrain our HMMs to have rectangular blocked emissions,

$$\mathbf{O} = \begin{bmatrix} \mathbf{O}^1 & 0 & 0 \\ 0 & \dots & 0 \\ 0 & 0 & \mathbf{O}^M \end{bmatrix}$$

where each $\mathbf{O}_m \in \mathbb{R}^{k \times |\mathcal{X}_m|}$ ($k = |\mathcal{Z}|/M$) is a partition indicating which tokens \mathcal{X}_m can be emitted

² Quasi-RNNs (Bradbury et al., 2016) also have a logarithmic dependency on T by applying the same prefix-sum trick, but do not model uncertainty over latent dynamics.

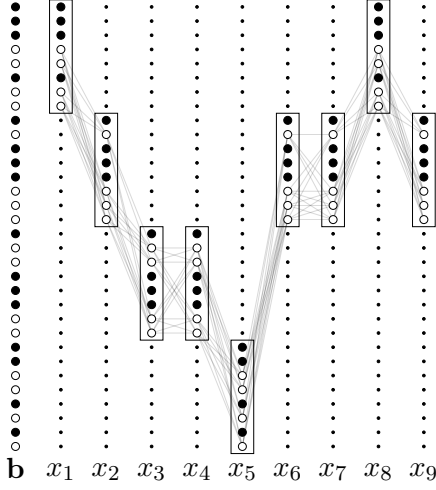


Figure 2: Computation of $p(\mathbf{x})$ is greatly reduced by blocked emissions and state dropout. Edges between nodes in the trellis indicate nonzero transition probabilities after clamping potentials with \mathbf{x} .

by states mk through $(m+1)k$. Conversely let $\mathcal{Z}_x \subset \mathcal{Z}$ be the states with non-zero probability of emitting x (with $|\mathcal{Z}_x| = k$). Exact marginalization can be computed via

$$p(\mathbf{x}) = \sum_{z_1 \in \mathcal{Z}_{x_1}} p(z_1 | z_0) p(x_1 | z_1) \times \dots \sum_{z_T \in \mathcal{Z}_{x_T}} p(z_T | z_{T-1}) p(x_T | z_T) \quad (3)$$

This gives a serial complexity of $O(T(|\mathcal{Z}|/M)^2)$.

Factored Neural Parameterization Even with blocked emissions, the scalar parameterization of an HMM grows as $O(|\mathcal{Z}|^2)$. We instead employ a neural parameterization. The approach is to embed each state in \mathcal{Z} ($\mathbf{E}_z \in \mathbb{R}^{|\mathcal{Z}| \times h/2}$), each token in \mathcal{X} ($\mathbf{E}_x \in \mathbb{R}^{|\mathcal{X}| \times h}$), and each block ($\mathbf{E}_m \in \mathbb{R}^{M \times h/2}$). From these we can create representations for leaving and entering a state, and emitting a word:

$$\mathbf{H}_{\text{out}}, \mathbf{H}_{\text{in}}, \mathbf{H}_{\text{emit}} = \text{MLP}(\mathbf{E}_m, \mathbf{E}_z)$$

The HMM distributional parameters are given by,

$$\phi = \mathbf{H}_{\text{emit}} \mathbf{E}_x^\top \quad \psi = \mathbf{H}_{\text{in}} \mathbf{H}_{\text{out}}^\top \quad (4)$$

where $\phi \in \mathbb{R}^{|\mathcal{Z}| \times |\mathcal{X}|}$ and $\psi \in \mathbb{R}^{|\mathcal{Z}| \times |\mathcal{Z}|}$. The MLP architecture follows (Kim et al., 2019), with details in the appendix. This neural parameterization takes $O(h^2 + h|\mathcal{Z}| + h|\mathcal{X}|)$ parameters (shown in Figure 1).

Note that parameter computation is independent of inference and can be cached completely at test-time. For training, we compute them once per batch

Algorithm 1 HMM Training (a single batch)

Given: block structure and model parameters
 Sample block-wise dropout mask \mathbf{b}
 Compute ϕ, ψ ignoring $b_z = 0$
for all examples \mathbf{x} in batch **do**
 $\Phi = \text{LOGPOTENTIALS}(\phi, \psi, \mathbf{x}, \mathbf{b})$
 $\log p(\mathbf{x}) = \text{FORWARD}(\Phi)$
 Update embeddings $\mathbf{E}_z, \mathbf{E}_x, \mathbf{E}_\pi$

(shown in Alg 1), while RNNs and similar models recompute emissions every token.

Dropout as State Reduction To encourage full use of the state space, we introduce dropout that prevents the model from favoring specific states. We propose a form of HMM state dropout that removes states from use entirely, which has the added benefit of speeding up inference.

State dropout acts on each emission block $\mathbf{O}_1, \dots, \mathbf{O}_M$ independently. For each block (with $k = |\mathcal{Z}|/M$ rows), we sample a binary dropout mask by sampling λk dropped row indices uniformly without replacement, where λ is the dropout rate. We concatenate these to a global vector \mathbf{b} , which, along with the previous constraints, ensures,

$$p(x | z) \propto b_z 1(z \in \mathcal{Z}_x) e^{\phi_{zx}} \quad (5)$$

State dropout gives a large practical speed up for both parameter computation and inference. For $\lambda = 0.5$ we get a $4\times$ speed improvement for both, due to reduction of possible transitions. This structured dropout is also easy to exploit on GPU, as it maintains block structure with fixed-height (as shown in Figure 2).

5 Experimental Setup

Emission Blocks The model requires partitioning token types into blocks \mathcal{X}_m . While there are many partitioning methods, a natural choice is Brown clusters (Brown et al., 1992; Liang, 2005) which are also based on HMMs. Brown clusters are obtained by assigning every token type in \mathcal{X} a state in an HMM, then merging states until a desired number of partitions M is reached. We construct the Brown clusters on the training portions of the datasets.

Datasets We evaluate on the Penn Treebank (Marcus et al., 1993) (929k train tokens, 10k vocab) and wikitext2 (Merity et al., 2016) (2M train to-

Model	Param	Val	Test
Penn Treebank			
KN 5-gram	2M	-	141.2
AWD-LSTM	24M	60.0	57.3
256 FF 5-gram	2.9M	159.9	152.0
2x256 dim LSTM	3.6M	93.6	88.8
HMM+RNN	10M	142.3	-
HMM ($ \mathcal{Z} =900$)	10M	284.6	-
VL-NHMM ($ \mathcal{Z} = 2^{15}$)	7.7M	125.0	115.8
WikiText			
KN 5-gram	5.7M	248.7	234.3
AWD-LSTM	33M	68.6	65.8
256 FF 5-gram	8.8M	210.9	195.0
2x256 LSTM	9.6M	124.5	117.5
VL-NHMM ($ \mathcal{Z} = 2^{15}$)	13.7M	169.0	158.2

Table 1: Perplexities on the PTB / Wikitext-2.

kens, 33k vocab) datasets. For Penn Treebank we use the preprocessing from Mikolov et al. (2011), which lowercases all words and substitutes OOV words with unks. For Wikitext2 casing is preserved, and all OOV words are unked.

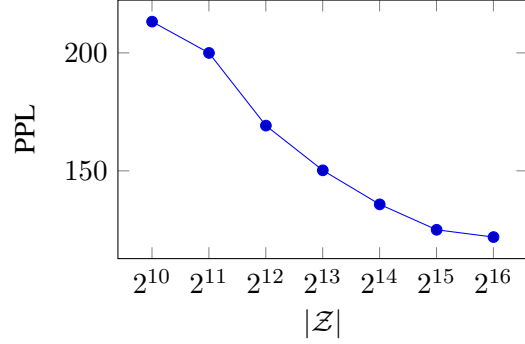
Baselines Baselines include AWD-LSTM (Merity et al., 2017); a 900-state scalar HMM and HMM+RNN extension, which discards the HMM assumptions (Buys et al., 2018); a KN 5-gram model (Mikolov and Zweig, 2012; Heafield et al., 2013), a 256 dimension FF model, and a 2-layer 256 dimension LSTM. We compare these with our very large neural HMM (VL-NHMM, $|\mathcal{Z}| = 2^{15}$) which has 2^{15} total states but only considers 256 states at every timestep at test time.³ See the appendix for all hyperparameters.

6 Results

Table 1 gives the main results. On PTB, the VL-NHMM is able achieve 125.0 perplexity on the valid set, outperforming a FF baseline (159.9) and vastly outperforming the 900-state HMM from Buys et al. (2018) (284.6).⁴ The VL-NHMM also outperforms the HMM+RNN extension of Buys et al. (2018) (142.3). These results indicate that HMMs are a much stronger model on this bench-

³ The 256 dim FF, LSTM, and VL-NHMM in particular have comparable computational complexity: $O(256^2T)$.

⁴ Buys et al. (2018) only report validation perplexity for the HMM and HMM+RNN models, so we compare accordingly.

Figure 3: Perplexity on PTB by state size $|\mathcal{Z}|$ ($\lambda = 0.5$ and $M = 128$).

Model	Param	Train	Val	Time
VL-NHMM (2^{14})	5.6M	122	136	48
- neural param	423M	119	169	14
- dropout	5.6M	89	145	100
- block emb	7.2M	115	134	40

Table 2: Ablations on PTB ($\lambda = 0.5$ and $M = 128$). Time is ms per eval batch (Run on RTX 2080).

mark than previously claimed. However, the VL-NHMM is outperformed by LSTMs. This trend persists in Wikitext-2, with the VL-NHMM outperforming the FF model but underperforming an LSTM.

Fig. 3 examines the effect of state size: We find that performance continuously improves significantly as we grow to 2^{16} states.

Table 2 considers other ablations: Although neural and scalar parameterizations reach similar training perplexity, the neural model generalizes better on validation with almost 100x fewer parameters. We find that state dropout results in both an improvement in perplexity and a large improvement in computation.

7 Conclusion

This work demonstrates that scaling HMMs to large states spaces results in performance gains. We make three contributions: a blocked emission constraint, a neural parameterization, and state dropout, which lead to an HMM that outperforms n-gram models and prior HMMs. This work demonstrates that classic HMMs can scale on modern hardware, and are worthy of consideration for NLP tasks.

References

- Yoshua Bengio, Réjean Ducharme, Pascal Vincent, and Christian Janvin. 2003. A neural probabilistic language model. *J. Mach. Learn. Res.*, 3(null):1137–1155.
- James Bradbury, Stephen Merity, Caiming Xiong, and Richard Socher. 2016. [Quasi-recurrent neural networks](#). *CoRR*, abs/1611.01576.
- Peter F. Brown, Peter V. deSouza, Robert L. Mercer, Vincent J. Della Pietra, and Jenifer C. Lai. 1992. Class-based n-gram models of natural language. *Comput. Linguist.*, 18(4):467–479.
- Jan Buys, Yonatan Bisk, and Yejin Choi. 2018. Bridging hms and rnns through architectural transformations.
- Tianqi Chen, Thierry Moreau, Ziheng Jiang, Haichen Shen, Eddie Q. Yan, Leyuan Wang, Yuwei Hu, Luis Ceze, Carlos Guestrin, and Arvind Krishnamurthy. 2018. [TVM: end-to-end optimization stack for deep learning](#). *CoRR*, abs/1802.04799.
- Antoine Dedieu, Nishad Gothoskar, Scott Swingle, Wolfgang Lehrach, Miguel Lázaro-Gredilla, and Dileep George. 2019. [Learning higher-order sequential structure with cloned hms](#).
- Wenjuan Han, Yong Jiang, and Kewei Tu. 2017. [Dependency grammar induction with neural lexicalization and big training data](#). In *Proceedings of the 2017 Conference on Empirical Methods in Natural Language Processing*, pages 1683–1688, Copenhagen, Denmark. Association for Computational Linguistics.
- Kenneth Heafield, Ivan Pouzyrevsky, Jonathan H. Clark, and Philipp Koehn. 2013. [Scalable modified Kneser-Ney language model estimation](#). In *Proceedings of the 51st Annual Meeting of the Association for Computational Linguistics (Volume 2: Short Papers)*, pages 690–696, Sofia, Bulgaria. Association for Computational Linguistics.
- Zhongqiang Huang. 2011. [Modeling Dependencies in Natural Languages with Latent Variables](#). Ph.D. thesis, University of Maryland.
- Yoon Kim, Chris Dyer, and Alexander M. Rush. 2019. [Compound probabilistic context-free grammars for grammar induction](#). *CoRR*, abs/1906.10225.
- Viktoria Krakovna and Finale Doshi-Velez. 2016. [Increasing the interpretability of recurrent neural networks using hidden markov models](#).
- Thomas Kuhn, Heinrich Niemann, and Ernst Günter Schukat-Talamazzini. 1994. [Ergodic hidden markov models and polygrams for language modeling](#). pages 357–360.
- Richard E. Ladner and Michael J. Fischer. 1980. [Parallel prefix computation](#). *J. ACM*, 27(4):831–838.
- Percy Liang. 2005. Semi-supervised learning for natural language. In *MASTER’S THESIS, MIT*.
- Ilya Loshchilov and Frank Hutter. 2017. [Fixing weight decay regularization in adam](#). *CoRR*, abs/1711.05101.
- Mitchell P. Marcus, Beatrice Santorini, and Mary Ann Marcinkiewicz. 1993. [Building a large annotated corpus of English: The Penn Treebank](#). *Computational Linguistics*, 19(2):313–330.
- Stephen Merity, Nitish Shirish Keskar, and Richard Socher. 2017. [Regularizing and optimizing LSTM language models](#). *CoRR*, abs/1708.02182.
- Stephen Merity, Caiming Xiong, James Bradbury, and Richard Socher. 2016. [Pointer sentinel mixture models](#). *CoRR*, abs/1609.07843.
- T. Mikolov and G. Zweig. 2012. Context dependent recurrent neural network language model. In *2012 IEEE Spoken Language Technology Workshop (SLT)*, pages 234–239.
- Tomas Mikolov, Anoop Deoras, Stefan Kombrink, Lukás Burget, and Jan Cernocký. 2011. [Empirical evaluation and combination of advanced language modeling techniques](#). pages 605–608.
- Slav Petrov, Leon Barrett, Romain Thibaux, and Dan Klein. 2006. [Learning accurate, compact, and interpretable tree annotation](#). page 433–440.
- Lawrence R. Rabiner. 1990. *A Tutorial on Hidden Markov Models and Selected Applications in Speech Recognition*, page 267–296. Morgan Kaufmann Publishers Inc., San Francisco, CA, USA.
- Ke M. Tran, Yonatan Bisk, Ashish Vaswani, Daniel Marcu, and Kevin Knight. 2016. [Unsupervised neural hidden markov models](#). *CoRR*, abs/1609.09007.
- Stephan Vogel, Hermann Ney, and Christoph Tillmann. 1996. [Hmm-based word alignment in statistical translation](#). In *Proceedings of the 16th Conference on Computational Linguistics - Volume 2, COLING ’96*, page 836–841, USA. Association for Computational Linguistics.
- Sam Wiseman, Stuart M. Shieber, and Alexander M. Rush. 2018. [Learning neural templates for text generation](#). *CoRR*, abs/1808.10122.
- Wojciech Zaremba, Ilya Sutskever, and Oriol Vinyals. 2014. [Recurrent neural network regularization](#). *CoRR*, abs/1409.2329.

A Appendices

A.1 Hyperparameters

For Penn Treebank and Wikitext-2, we trained the following baselines: a two layer feed-forward 256-dim 5-gram model and a two layer 256-dim LSTM. The feedforward model is given by the following:

$$p(w_t | \mathbf{w}_{<t}) = W_x \text{ReLU}(\text{Conv}(\mathbf{E}_w(\mathbf{w}_{t-4:t-1}))) \quad (6)$$

where \mathbf{E}_w gives the word embeddings and $W_x \in \mathbb{R}^{|\mathcal{X}| \times h}$ is weight-tied to the embeddings.

For the (5-gram) feedforward model we use a batch size of 128 and a bptt length of 64, as we found the model needed a larger batch size to achieve decent performance. For the LSTM, we use a batch size of 16 and a BPTT length of 32. For both baseline models we use AdamW (Loshchilov and Hutter, 2017) with a learning rate of 1e-3 and a dropout rate of 0.3 on the activations in the model. Both models use a hidden dimension of 256 throughout. These same hyperparameters were applied on both Penn Treebank and Wikitext-2.

For the HMMs we use a batch size of 16 and a BPTT length of 32. We use state dropout with $\lambda = 0.5$. We use AdamW (Loshchilov and Hutter, 2017) with a learning rate of 1e-2 for Penn Treebank, and a learning rate of 1e-3 for Wikitext-2.

All weights are initialized with the Kaiming uniform initialization. The FF model was trained for 100 epochs, while all other models were trained for 50. Validation likelihood was checked 4 times per epoch, and learning rates were decayed by a factor of 4 if the validation performance did not improve after 8 checks.

Hyperparameter search was performed manually, using the best validation perplexity achieved in a run. Bounds:

1. Learning rate $\in \{0.0001, 0.001, 0.01, 0.1\}$
2. Dropout $\lambda \in \{0, 0.25, 0.5, 0.75\}$
3. Hidden dimension $h \in \{128, 256, 512\}$
4. Batch size $\in \{16, 32, 64, 128\}$

Experiments were run on RTX 2080 GPUs.

On PTB the FF model takes 3s per epoch, the LSTM 23s, and the VL-HMM 2^{15} 433s. The inference for VL-HMM has not heavily optimized,

Constraint	$ \mathcal{Z} $	$ \mathcal{C}_x $	m	Val PPL
Brown	16384	512	32	137
Brown	16384	256	64	138
Brown	16384	128	128	134
Brown	16384	64	256	136
None	1024	-	-	180
Brown	1024	256	4	182
Brown	1024	128	8	194
Uniform	8192	128	-	150
Brown	8192	128	64	142
Uniform	16384	128	-	146
Brown	16384	128	128	136

Table 3: Emission constraint ablations on Penn Treebank.

and uses a kernel produced by TVM (Chen et al., 2018) for computing gradients through marginal inference.

A.2 HMM Parameterization

Let $\mathbf{E}, \mathbf{D} \in \mathbb{R}^{v \times h}$ be an embedding matrix and a matrix of the same size, where v is the size of the vocab and h the hidden dimension. We use the following residual network:

$$\begin{aligned} f_i(\mathbf{E}) &= g_i(\text{ReLU}(\mathbf{E}W_{i1})) \\ g_i(\mathbf{D}) &= \text{LayerNorm}(\text{ReLU}(\mathbf{D}W_{i2}) + \mathbf{D}) \end{aligned} \quad (7)$$

with $i \in \{\text{out}, \text{in}, \text{emit}\}$, $W_{i1}, W_{i2} \in \mathbb{R}^{h \times h}$ where h is the hidden dimension.

For the factored state embeddings in Sec. 4, we introduce residual networks $f_j, j \in \{o, i, e\}$ to compose block and state embeddings, yielding

$$\begin{aligned} \mathbf{H}_{\text{out}} &= f_{\text{out}}(f_o([\mathbf{E}_m, \mathbf{E}_z])) \\ \mathbf{H}_{\text{in}} &= f_{\text{in}}(f_i([\mathbf{E}_m, \mathbf{E}_z])) \\ \mathbf{H}_{\text{emit}} &= f_{\text{emit}}(f_e([\mathbf{E}_m, \mathbf{E}_z])) \end{aligned} \quad (8)$$

A.3 Emission Constraint Ablation

Tbl. 3 shows the results from emission constraint ablations. For the ablations in this section, we do not use the factored state embedding and instead directly learn embeddings $\mathbf{E}_z \in \mathbb{R}^{|\mathcal{Z}| \times h}$. We examine the effect of factored state embeddings in the next section.

With a VL-NHMM that has $|\mathcal{Z}| = 2^{14}$ states, the model is insensitive to the number of blocks

M . However, with fewer states $|\mathcal{Z}| = 2^{10}$ where we are able to use fewer blocks to examine whether the block-sparsity of the emission results in a performance loss. With $M = 4$ blocks, the block-sparse HMM matches an unconstrained HMM with the same number of states. When $M = 8$, the block-sparse model underperforms, implying there may be room for improvement with the larger HMMs that use $M > 8$ blocks.

We additionally compare the blocks induced by Brown clustering with a uniform constraint that samples subsets of states of size n independently and uniformly from \mathcal{Z} . This does not admit a partitioning, which makes it difficult to apply state dropout. We therefore zero out half of the logits of the transition matrix randomly before normalization. In the bottom of Tbl. 3, we find that models with uniform constraints are consistently outperformed by models with Brown cluster constraints as measured by validation perplexity. The models with uniform constraints also had poor validation performance despite better training performance, a symptom of overfitting.

These ablations demonstrate that the constraints based on Brown clusters used in this work may not be optimal, motivating future work that learns sparsity structure.

A.4 Factored State Representation Ablation

We examine the effect of factoring state representations into block embeddings and independent state embeddings. Recall that factored state representations were parameterized via

$$\mathbf{H}_{\text{out}}, \mathbf{H}_{\text{in}}, \mathbf{H}_{\text{emit}} = \text{MLP}(\mathbf{E}_m, \mathbf{E}_z)$$

with the block and state embeddings $\mathbf{E}_m, \mathbf{E}_z \in \mathbb{R}^{|\mathcal{Z}| \times h/2}$. We ablate this by comparing to the following independent state representation:

$$\mathbf{H}_{\text{out}}, \mathbf{H}_{\text{in}}, \mathbf{H}_{\text{emit}} = \mathbf{E}'_z$$

with $\mathbf{E}'_z \in \mathbb{R}^{|\mathcal{Z}| \times h}$. The results of the factored state ablation are in Fig. 4,

We find that the performance of independent state embeddings is similar to a model with factored embeddings, until the number of blocks is ≤ 64 .

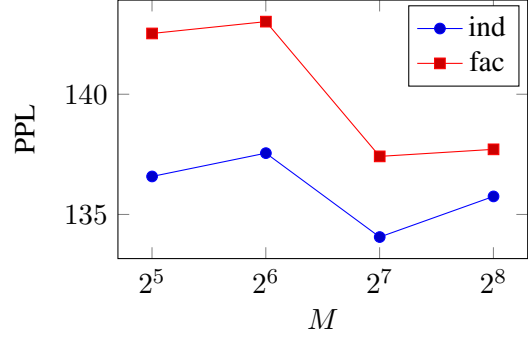


Figure 4: Perplexity on PTB by number of blocks M ($\lambda = 0.5$ and $|\mathcal{Z}| = 2^{14}$).

Model	Size	Train	Val	Time
VL-NHMM (2^{14})	5.6M	122	136	48
- neural param	423M	119	169	14
- dropout	5.6M	89	145	100
- block emb	7.2M	115	134	40

Table 4: Ablations on PTB ($\lambda = 0.5$ and $M = 128$). Time is ms per eval batch (Run on RTX 2080).

A.5 Computational Considerations

We reproduce the technique ablation table here in Tbl. 4 for reference. As we remove neural components, the number of parameters increases but the time of the forward pass decreases. This is because generating parameters from a neural network takes strictly more time than having those parameters available, similar to a hierarchical Bayesian model.

When block embeddings are removed and the state representations are directly parameterized, the model is faster due to not needing to recompute state representations. This contrast is even more pronounced when removing neural components altogether, with an almost 3x speedup. However, we note that the drop in generalization is large, indicating the neural parameterization helps with learning. Therefore we use the neural parameterization at training time, then cache the resulting HMM parameters (the transition and emission matrices) for use during inference.